ACS OMEGA

Article

Cite This: ACS Omega 2018, 3, 3096−3103

Rapid Accessible Fabrication and Engineering of Bilayered Hydrogels: Revisiting the Cross-Linking Effect on Superabsorbent Poly(acrylic acid)

Kyoung Min Lee,[†,‡] Hea Ji Kim,[†] Doyoung Jung,[†] Yuree Oh,[†] Hyemin Lee,[§] Changsun Han,[§] Ji Young Chang,[*,‡] and Hyungwoo Kim[*,†]

[†]School of Polymer Science and Engineering, Chonnam National University, Gwangju 61186, Korea

[‡]Department of Materials Science and Engineering, College of Engineering, Seoul National University, Seoul 08826, Korea

[§]Basic Materials and Chemicals R&D, LG Chem, Ltd, R&D Campus Daejeon, 188 Moonji-ro, Yuseong-gu, Daejeon 34122, Korea

Supporting Information

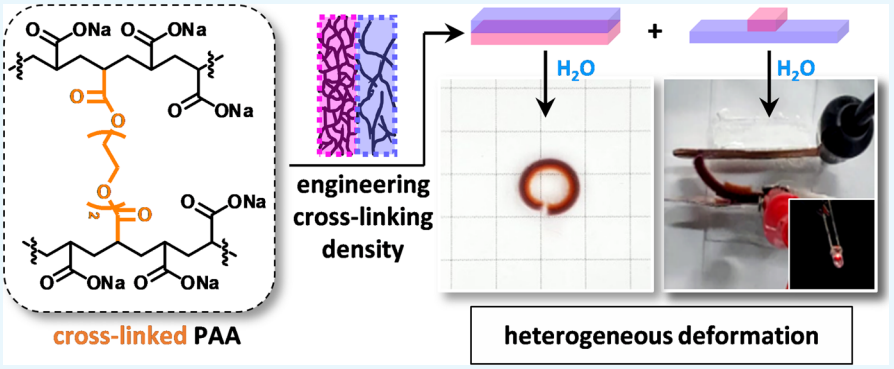

ABSTRACT: Superabsorbent hydrogels are significant not only in materials science but also in industries and daily life, being used in diapers or soil conditioners as typical examples. The main feature of these materials is their capacity to hold considerable amount of water, which is strongly dependent on the cross-linking density. This study focuses on the preparation of hydrogels by reweighing the effect of cross-linking density on physical properties, which provides green fabrication of bilayered hydrogels that consist of homogeneous structural motifs but show programmed responses via sequential radical polymerization. In particular, when two hydrogel layers containing different cross-linking densities are joined together, an integrated linear bilayer shows heterogeneous deformation triggered by water. We monitor the linear hydrogel bilayer bending into a circle and engineer it by incorporating disperse dyes, changing colors as well as physical properties. In addition, we demonstrate an electric circuit switch using a patterned hydrogel. Anisotropic shape change of the polyelectrolyte switch closes an open circuit and lights a light-emitting diode in red. This proposed fabrication and engineering can be expanded to other superabsorbent systems and create smart responses in cross-linked systems for biomedical or environmental applications.

INTRODUCTION

Since poly(2-hydroxyethyl methacrylate) was reported to form a hydrogel in the presence of a cross-linker,[1] a myriad of hydrogels have been widely researched for biomedical and environmental purposes. Among them, superabsorbent hydrogels (SHs) confine considerable amount of water into a three-dimensional, cross-linked network, which is typically greater than hundreds to thousands times their dry weight, and swell while maintaining the original shape.[2−4] Acrylic acid (or acrylate) and acrylamide are extensively used as monomers, along with other monomers such as *N*-isopropylacrylamide, *N*,*N*-diethylacrylamide, and more interestingly, bioextractable sodium 4-hydroxy-2-methylenebutanoate[5] or polymers including poly(vinyl alcohol), which are further cross-linked covalently or noncovalently in situ or ex situ.[2,6] When exposed to aqueous conditions, hydrophilic groups in the polymer network are primarily hydrated by water molecules, and then, the additional water can be absorbed via capillary force and osmotic pressure for filling the space inside the network. Such wet materials essentially possess small yet functionally crucial cross-linking density, which not only leads to water absorbency but also modulates the physical properties of the entire material on demand, for example, elasticity or swelling ratio.

The versatility of SHs has offered privileged, sustainable applications. For instance, from the perspective of polymeric materials, swellable materials have been used as elastomers, watery matrices, containers, supports, and films, which can be further applied in many fields such as soil conditioning, tissue

Received: January 15, 2018
Accepted: March 5, 2018
Published: March 14, 2018

DOI: 10.1021/acsomega.8b00079
ACS Omega 2018, 3, 3096−3103

engineering, desalination, catalysis, and health care.[6] In particular, stimuli-responsive SHs have gained notable interest because of the following characteristics:[7−21] (i) bio- and environmental compatibility, (ii) wide range of functional monomers/building blocks including cost-effective natural products (e.g., cellulose, alginate, starch, chitosan, polysaccharides, and proteins), (iii) possible use of water as an eco-friendly ubiquitous stimulus, (iv) use of a broad library of well-established chemistry for synthesis, for example, radical polymerizations, (v) distinguishable volumetric change, and (vi) processability into smart composites integrated with inorganic components that render synergy effects via hybridization. Besides, responsive SHs have been remarkably used as a hydrogel actuator under aqueous conditions. The materials show reconfigurable shape changes in response to pH,[22] temperature,[23−25] salinity,[26] metal ions,[27,28] light,[29] or electric potential,[30,31] taking one step forward to biomimetic responses.

In this study, we demonstrate a green fabrication method of bilayered hydrogels that show heterogeneous deformation under aqueous conditions by controlling the cross-linking density. The bilayer structure consists of homogeneous chemical species (i.e., cross-linked poly(acrylic acid)) and enables low-cost effort-saving fabrication through sequential radical polymerization in water without the need of ancillary adhesives—eliminating possible interfacial complexity that raises the outbreak of debonding. Instead, only the gap in cross-linking density significantly alters the physical properties of hydrogels, building up programmed responses of the bilayer. Therefore, we evaluate the effect of cross-linking density on superabsorbency, mechanical strength, and thermal stability of hydrogels, which allows a controlled deformation triggered by water. As designed, the bilayered hydrogel curls into a circle when wet; the behavior is dependent on pH. Each layer can be colored with disperse dyes for visual clarity, and the bilayer exhibits material properties emanating from both layers. Furthermore, we prepare a circuit switch using a patterned hydrogel. A small firmly cross-linked hydrogel patch induces enough hydraulic force to bend the loosely cross-linked hydrogel strip, which closes the circuit and switches on a light-emitting diode (LED).

RESULTS AND DISCUSSION

Fabrication of a Hydrogel Film from a Glass Template via Radical Polymerization. Figure 1 shows the synthetic procedure of a poly(acrylic acid)-based hydrogel film under aqueous conditions by radical polymerization. First, acrylic acid (14 mL) was added to water (8 mL). Two phases were separated initially, but 80% neutralization with NaOH gave a homogeneous solution with a molar concentration of 8 mM. Then, di(ethylene glycol) acrylate (cross-linker) and potassium persulfate (KPS) (initiator) were added to provide a ready-to-polymerize solution, which was transferred by a syringe to a glass template having a rectangular space inside (11.5 cm × 15 cm × 0.1 cm) for polymerization. The template had a high ratio of surface area to volume and could facilitate efficient heat transfer, which is similar to controlling autoacceleration process in the sheet-type mold. After the displacement, the monomer solution was polymerized on a heating plate at a set temperature of 55 °C for 2 h; the cross-linked hydrogel film was obtained and unloaded from the mold. The soft film was even and transparent without the inclusion of severe cavitation and had a size similar to that of the template. The chemical structure of the hydrogel is shown in the inset of Figure 1.

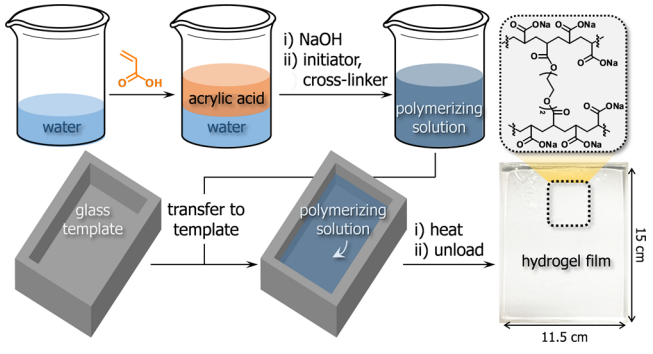

Figure 1. Schematic description for the preparation of a poly(acrylic acid)-based hydrogel film. The neutralized monomer was polymerized in a glass template. The transparent hydrogel film obtained and its cross-linked chemical structure are shown in the inset.

Effect of Cross-Linking on the Swelling Properties. A poly(acrylic acid) film dramatically absorbs water and shows a distinct size expansion while maintaining its initial shape. During swelling, the diacrylate cross-linker in the hydrogel films fundamentally affected the superabsorbency. As shown in Figure 2a, we prepared hydrogel films **1**−**6** containing different amounts of cross-linker under the same conditions, wet the films with deionized water, and expressed the effect of cross-linker on the absorbency by calculating the degree of swelling (eq 1) and cross-linking density (ρ) (eq 2) as follows:[32]

$$\text{Degree of swelling (\%)} = \frac{X - X_0}{X_0} \times 100 \quad (1)$$

where X indicates the weight of the wet analyte sample and X_0 is the weight of the sample dried under vacuum using a lyophilizer for 48 h.

$$\rho = -\frac{1}{V_{sol}}\left(\frac{\ln(1 - v_p) + v_p + \chi v_p^{\,2}}{v_p^{\,1/3} - 0.5 v_p}\right) \quad (2)$$

where V_{sol} indicates the molar volume of water; v_p is the equilibrium polymer volume fraction determined from the degree of swelling; and χ is the solvent−polymer interaction parameter of 0.46.[33]

The initial as-prepared samples had similar values for degree of swelling (44−47%), irrespective of the amount of cross-linker, because the films were consistently prepared from 0.8 M monomer solutions in water. However, after drying and re-swelling in water for 48 h, the hydrogel films showed different swelling ratios, which hinged on the cross-linking density. Film **2** (0.34 wt % of cross-linker) swelled for a maximum of 200 times, and then, the value decreased as more cross-linkers were involved. Figure 2b shows an isotropic dimensional change in **2**. The initial film had a side of 1.15 cm, which decreased by 26% when lyophilized, but exposure to water increased the side 4.1×. The black square behind the hydrogel film indicates the transparency of the film and supports the size estimation. As expected, the cross-linking density obtained from eq 2 revealed the inverse proportion against the swelling ratio of the films, except for the case of **1**, which has the least amount of cross-linker. We reason that the partially soluble loose network of **1** hindered the capillary force for water absorption.[34] In Figure 2c, the example porous network of **2** was observed using scanning electron microscopy (SEM), which was developed

DOI: 10.1021/acsomega.8b00079
ACS Omega 2018, 3, 3096−3103

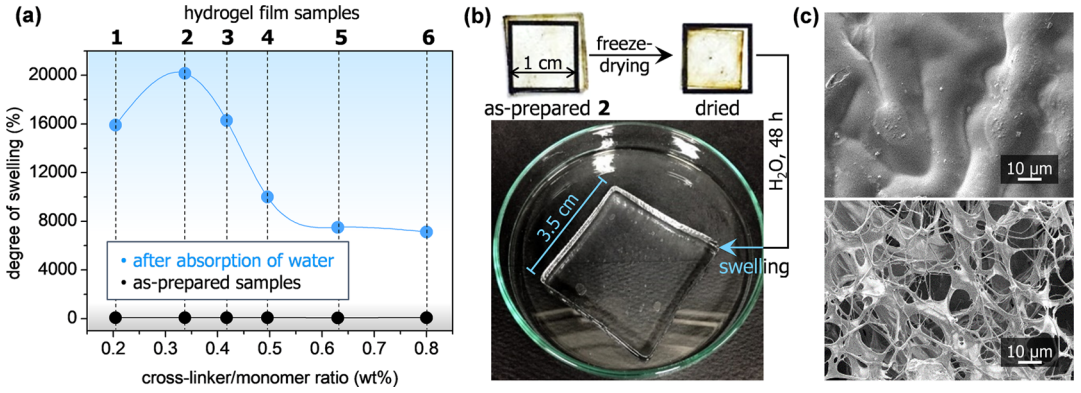

Figure 2. (a) Change in degree of swelling of hydrogel films with regard to the cross-linker ratio after immersing in water for 48 h (sky blue). The as-prepared samples contain a limited amount of water (44−47%) regardless of the ratio (black). (b) Representative volumetric change in film **2** when prepared and freeze-dried. The black square (area, 1 cm × 1 cm) helps to estimate the film size. After immersing in water for 48 h, the swelled film has a side that approximately measures 3.5 cm. (c) SEM images of as-prepared **2** (up) and after swelling in water for 48 h (down). Each sample was freeze-dried for 48 h before the measurement.

after swelling in water. The pore size ranges from 3 to 20 μm. All experimental values of the obtained hydrogels are summarized in Table 1.

Table 1. Degree of Swelling and Cross-Linking Density of Hydrogel Films 1−6

hydrogel film	cross-linker (wt %)	degree of swelling (%)	cross-linking density (mmol L^{-1})
1	0.20	15 912	0.71
2	0.34	20 164	0.47
3	0.42	16 287	0.68
4	0.50	10 011	1.55
5	0.63	7509	2.54
6	0.80	7140	2.77

In addition, we measured the actual change in the temperature of the polymerizing solution during radical polymerization. Therefore, a flexible thermocouple probe was inserted into the polymerizing solution of **2**, which was cast inside the template on a heating plate (set temperature, 55 °C), and the temperature was tracked by a digital thermometer, as shown in Figure 3a. The temperature exponentially increased for the initial 20 min and then slightly elevated more for 15 min, indicating an accelerated polymerization (Figure 3b). In general, Trommsdorff effect aggravates undesirable properties in polymeric materials, such as cavitation or unevenness, during polymerization.[35,36] However, the cast solution of **2** exhibited

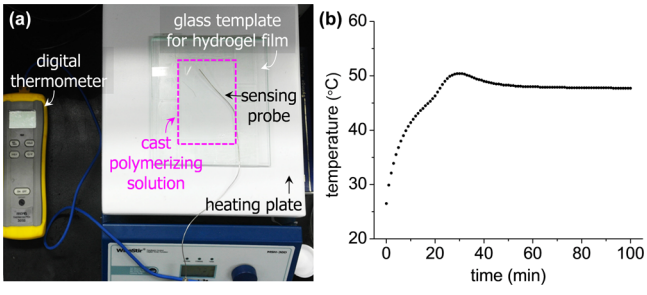

Figure 3. (a) Photograph of measuring temperature of the polymerizing solution of **2** in the glass template on a heating plate using a digital thermometer. (b) Change in the temperature of the solution during radical polymerization.

only a weak exothermic process, from which the regular hydrogel film **2** was produced. The maximum temperature was found to be 50.4 °C; thereafter, the temperature of the film was stabilized at 48 °C until the end of the reaction.

Effect of Cross-Linking on the Mechanical Strength of Hydrogels. Chemical cross-linking provides an effective approach to control the mechanical strength of polymeric materials. Herein, we measured the stress−strain curves of the resulting films, as shown in Figure 4. Figure 4a shows the representative curves for hydrogel samples **1**−**6**, from which we can anticipate the effect of cross-linking density. As described in Figure 4b, toughness values increased until the amount of cross-linker increased from 0.20 (film **1**) to 0.34 wt % (film **2**) and then decreased in inverse proportion to the amount of cross-linker. A similar tendency was observed for elongation at fracture. As an example, at 0.34 wt %, the toughness of film **2** was found to be 0.28 MJ m^{-3} with 300% elongation at fracture. On the other hand, Young's modulus only fluctuated within a narrow range of 0.12−0.15 MPa. Presumably, small change in cross-linker concentration would manipulate microstructures or induce microdeformation in hydrogels, leading to a change in ductility of materials rather than stiffness. We also changed the initiator concentration, which can control the molecular weight between the cross-links (M_c), another factor affecting the cross-linking density, during polymerization.[37,38] Thus, we polymerized film **2** using different initiator concentrations. Toughness increased in proportion to the amount of initiator until 0.56 wt % of KPS was incorporated (a maximum toughness, 0.40 MJ m^{-3}) and then decreased; in contrast, elongation at fracture decreased above 0.43 wt % (Figure S1). Although the total changes were much smaller than the results from the cross-linker concentration, a detailed future investigation would elaborate complementary effects of both factors on the mechanical properties of the hydrogel materials.

Furthermore, we took **1**, **3**, and **6** and measured their tensile strengths at 80 °C to investigate a thermal effect. At 80 °C, the films stiffened more—toughness and elastic modulus increased and elongation reduced—as compared to the measurement at 25 °C (Figure 5a−c). The total exposure time to heat during testing was less than 2 min. The fractured specimen from **3** (0.42 wt %) was hard and brittle, as shown in Figure S2b. To examine the effect of thermal treatment on hydrogels, we incubated film **3** at 40, 60, and 80 °C for 3 and 10 min and

DOI: 10.1021/acsomega.8b00079
ACS Omega 2018, 3, 3096−3103

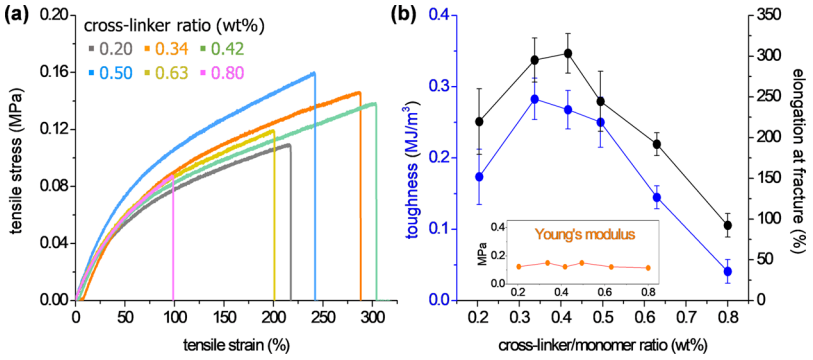

Figure 4. Mechanical properties of hydrogels **1**–**6**. (a) Representative tensile stress–strain curves from the hydrogels that contain different concentrations of cross-linker when polymerized with 0.25 wt % KPS. (b) Change in toughness (blue), elongation at fracture (black), and Young's modulus (orange, inset) of the hydrogels with respect to the concentration of cross-linker. The data points were obtained in quintuplicate from five independent experiments.

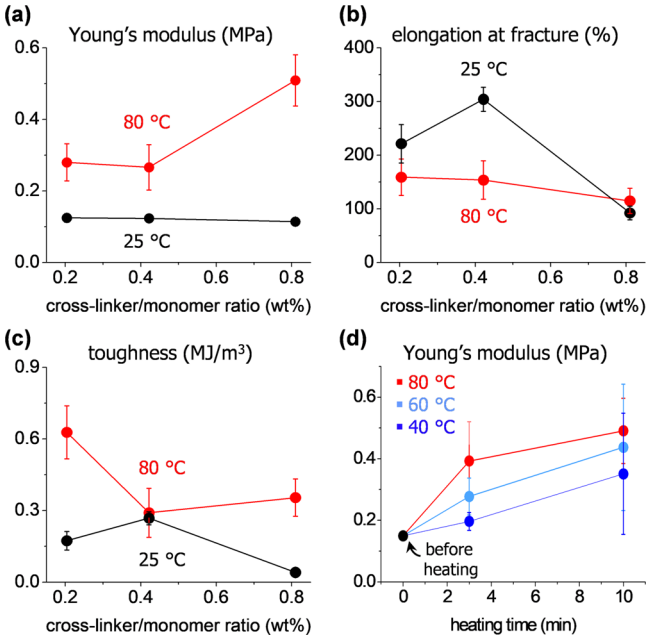

Figure 5. Young's modulus (a), elongation at fracture (b), and toughness (c) of hydrogel films **1**, **3**, and **6**, measured at 80 °C (red). The results from 25 °C (black) are shown for comparison. (d) Change in Young's modulus of **3** after exposure to different temperatures (40 °C, blue; 60 °C, sky blue; and 80 °C, red). The data points were obtained in quintuplicate from five independent experiments.

tested their mechanical strengths at the same temperatures (Figure 5d). The longer the exposure time at a higher temperature, the more rapidly did the Young's modulus increase, which indicates that the film hardened by thermal drying. On the other hand, potential thermal annealing would occur together inasmuch as the modulus gradually increased even at 40 °C less than the polymerizing temperature.[39]

Fabrication of Responsive Hydrogel Bilayers. A minor modification in the chemical structure (i.e., cross-linking density) alters the macroscopic physical properties of polymeric materials, highly encouraging us to develop responsive hydrogels capable of showing designed behaviors in water. In particular, when two adjacent parts with different cross-linking densities are joined together, the interface in between gives rise to heterogeneous deformation of the entire material, taking advantage of the different swelling ratios in an aqueous medium. Hence, we have designed and fabricated bilayered hydrogels by sequential radical polymerization (Figure 6a). In a glass template, we prepared the first layer containing 0.34 wt %

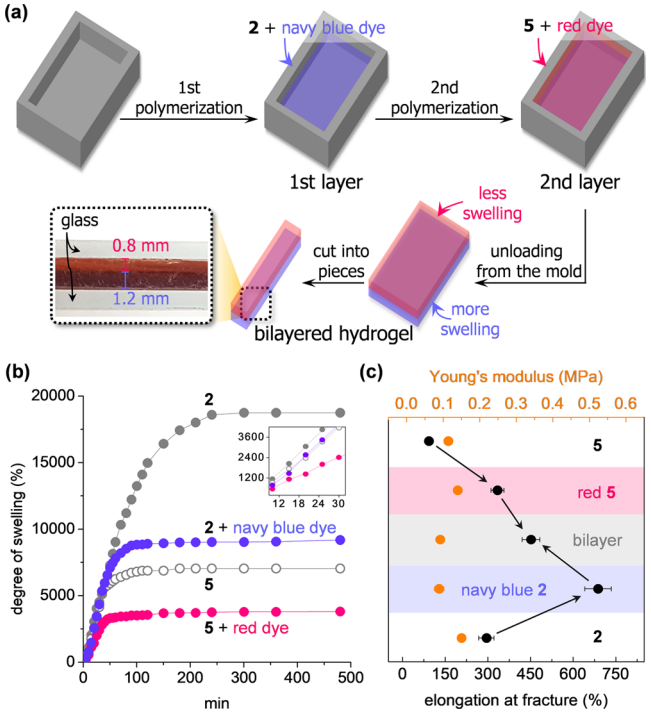

Figure 6. (a) Fabrication of the bilayered hydrogel via sequential polymerization. The first and second layers are prepared from **2** and **5** dyed in navy blue and red, respectively. (b) Change in the degree of swelling of each colored layer. Swelling behaviors of pristine **2** and **5** are shown for comparison, and the expanded view of the initial linear region is shown in the inset. (c) Change in elongation at fracture (black) and Young's modulus (orange) of hydrogels when dyed and integrated.

cross-linker (film **2**). On top, we directly deposited the second polymerizing solution containing 0.80 wt % cross-linker (film **5**) and polymerized under the same conditions in the presence of 0.25 wt % KPS. Each polymerizing solution was dyed with navy blue and red disperse dyes for differentiation before conducting polymerization. Therefore, in situ polymerization provided a bilayered structure of hydrogel in which the thickness of the first (navy blue) and second (red) layers measured 1.2 and 0.8 mm, respectively. The hydrogel layers

DOI: 10.1021/acsomega.8b00079
ACS Omega 2018, 3, 3096–3103

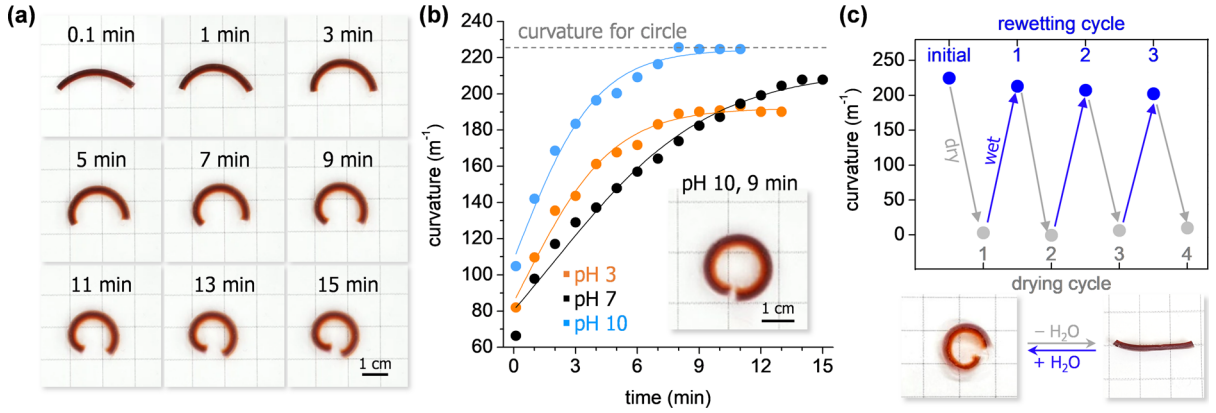

Figure 7. (a) Bending motion of the hydrogel in a pH 7 buffer solution at 25 °C. The linear bilayer curls into a round shape within 15 min. (b) Change in the curvature of the bilayer over time while exposed to buffer solutions of various pHs (pH 3, orange; pH 7, black; and pH 10, sky blue). A magnified image of the bilayer folding completely after immersed at pH 10 for 9 min is shown in the inset. (c) Change in the curvature of the bilayer during drying–rewetting cycles. Photographs of the bilayer taken at the third drying–rewetting cycle were presented.

adhered tightly to one another because of the probable interpenetration that would occur at the interface during the second polymerization reaction. After unloading from the glass mold, the bilayer was obtained, which had a volume of 2.8 cm × 0.2 cm × 0.3 cm and displayed an anisotropic shape change.

Figure 6b shows the change in the degree of swelling of each layer in deionized water, similarly determined by eq 2. Incorporated with the hydrophobic disperse dyes, the navy blue **2** and red **5** hydrogels exhibited a total degree of swelling that decreased in half when fully swelled, compared to **2** and **5** before dying. The insoluble dyes also affected the swelling rates of both hydrogel layers, which reduced from 193 to 177% min^{-1} for **2** and from 161 to 96% min^{-1} for **5** after dying, calculated from the linear slopes of the initial region (inset in Figure 6b). We further swapped the dyes in the layers, which yielded red **2** and navy blue **5** films. However, both samples showed less difference in the swelling ratios, meaning that the bilayer from navy blue **2** and red **5** can better induce the reconfiguration (Figure S3). Inclusion of the dyes also altered the mechanical strength of the hydrogel bilayer (Figure 6c). The hydrophobic dyes enhanced the elongation at fracture of **2** and **5**, which could sustain cross-linked structures during the elongation under tensile stress.[40] However, the bilayer displayed an average elongation at fracture of both hydrogels as expected, whereas the Young's modulus did not change much. Representative stress–strain curves are shown in Figure S4, and the measured values are listed in Table S5.

A designed behavior of bilayer is presented in Figure 7. Here, we investigated the bending of the bilayer in various pHs, which can affect the actuation of polyelectrolyte materials. Figure 7a shows the bilayer bending in a neutral pH 7 buffer. As soon as immersed in the buffer, the linear material bent in a round shape in 15 min, as the navy blue layer (**2**, 0.34 wt % cross-linker) that positioned outside swelled more than the red layer (**5**, 0.80 wt % cross-linker) inside. A longer exposure to the medium only increased the whole size of the bilayer to a small extent but did not unfold the shape (Figure S6). In addition, we investigated the effect of pH on the behavior of the hydrogel in aqueous media. Figure 7b reveals the change in the curvature of the deformed hydrogels when exposed to various pHs of 3, 7, and 10. The curvature of hydrogels autonomously increased as time elapsed. The curvature increased slightly faster (the rate of folding was found to be 28.1 m^{-1} s^{-1}, calculated from the initial linear region) at pH 3 than that at pH 7 (26.7 m^{-1} s^{-1}), but the final curvature was slightly lower than the value resulted from pH 7, accompanying less folding. Interestingly, the curvature increased most rapidly at pH 10 (rate, 33.6 m^{-1} s^{-1}; 1.3 times faster than that at pH 7), and the final curvature reached 224 m^{-1}—the theoretical curvature of a circle that has 2.8 cm circumference—in 9 min, as shown in the inset of Figure 7b. We assume that protonation of carboxylates at pH 3 could hinder a complete folding of the bilayer as decreasing hydrophilicity and water absorbency as well. However, the remaining acid groups would be deprotonated at pH 10, which could promote water absorbency and the following folding behavior while hydrophilicity increased. Time-lapsed photographs of the bending behavior are presented in Figures S5, S7, and S8. Furthermore, we tested the reversible shape change of the bilayer that was pre-exposed to pH 10 for 10 min. As expected, the curled bilayer recovered its original shape after taking away from water and drying under air for 1 h at 70 °C but bent again when rewet for 10 min at pH 10. During five drying–rewetting cycles, the bilayer iterated the programmed response without structural degeneration (Figure 7c).

In addition, we have engineered the hydrogel bilayer through patterning with glass masks (Figure 8a). The small glasses masked the first layer (navy blue **2**; size, 3 cm × 0.5 cm × 1.3 mm) during the second polymerization, leaving a small red patch (red **5**; size, 0.5 cm × 0.5 cm × 0.7 mm) on the bottom layer. The small patch caused the bending of the entire hydrogel in deionized water. We positioned the patterned hydrogel between two parallel copper plates, and the hydrogel was held onto the bottom plate with a crocodile clip. The copper plates were connected to an LED bulb and a dry cell battery, resulting in an open electronic circuit (Figure 8b). As designed, the hydrogel bending in deionized water touched the other copper plate 1 cm distant, closing the circuit. We could see a dim red light before deformation because the hydrogel contains charged ions, which would diffuse into deionized water. However, the underwater actuation lit the LED bulb in bright red in 2 min (Figure 8c).

CONCLUSIONS

Bilayered hydrogels capable of showing programmed responses have been demonstrated. The hydrogels are made by cross-linking superabsorbent poly(acrylic acid), where cross-linking density plays a crucial role in manipulating the swelling

DOI: 10.1021/acsomega.8b00079
ACS Omega 2018, 3, 3096–3103

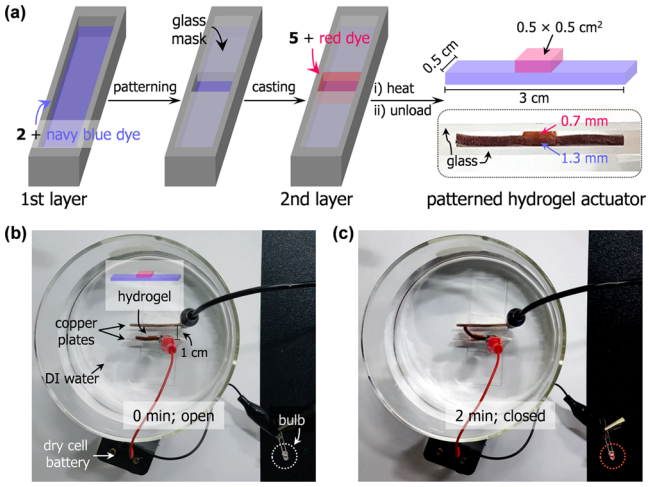

Figure 8. (a) Depiction for fabrication of the patterned hydrogel. The glass masks are placed on the first layer in situ before casting the second polymerizing solution. The first and second layers are prepared from the same solutions as those used in Figure 6. (b,c) Circuit switch based on the patched hydrogel (b, open circuit). In deionized water, the bending hydrogel connects two plates, switching on the LED in red (c, closed circuit).

behavior as well as mechanical strength. In particular, engineering cross-linking density provides heterogeneous deformation when two SHs containing different cross-linking densities are consolidated via sequential in situ polymerization. Through the rapid accessible fabrication, we were able to prepare bilayered hydrogels and colored each layer with disperse dyes. The concomitant physical changes were investigated. The linear hydrogel bilayer revealed a pH-dependent folding behavior and showed remarkably fast complete deformation at pH 10. Furthermore, patterning on the hydrogel brought about a polyelectrolyte switch that closed the circuit and lit an LED bulb in red. This fabrication method can be expanded to other superabsorbent systems using biocompatible monomers, and a merger with diverse functionalities would expedite the development of cross-linked polymeric systems that feature smart responses for many biomedical or eco-friendly applications, for example, micro-lenses that show a controlled release or functional membranes that remove specific pollutants (e.g., microplastics) in the ocean.

EXPERIMENTAL SECTION

Materials. Acrylic acid, di(ethylene glycol)diacrylate, and KPS were obtained from Sigma-Aldrich. Disperse dyes such as Synolon N/Blue S-GLS (navy blue color) and Synolon Rubine S-GEL (red color) were purchased from Kimco. Acrylic acid was distilled under reduced pressure at 50 °C before use. Deionized water was prepared using a water purification system (Pure Power I+, DAIHAN Scientific). All other reagents and solvents used were purchased commercially and were used as received unless otherwise noted.

Analytical Methods. For nuclear magnetic resonance (NMR) measurement, hydrogel sample **2** was prepared in an NMR tube using D_2O instead of water. ^{1}H NMR spectrum was recorded using a Bruker 300 MHz NMR spectrometer at 25 °C. Proton chemical shifts are expressed in parts per million (ppm, δ scale) and are referenced to tetramethylsilane ($(CH_3)_4Si$, δ 0.00 ppm) or to residual protium in the solvent (D_2O, δ 4.70 ppm). Data are represented as follows: chemical shift, multiplicity (s = singlet, d = doublet, t = triplet, q = quartet, m = multiplet and/or multiple resonances, and br = broad peak), integration. Carbon nuclear magnetic resonance (^{13}C NMR) was recorded using a Bruker 500 MHz NMR spectrometer at 25 °C. Carbon chemical shifts are expressed in parts per million (ppm, δ scale) and are referenced to tetramethylsilane ($(CH_3)_4Si$, δ 0.00 ppm). For the tensile test, the as-prepared hydrogel films were cut using a laser cutter. The films were glued between two PMMA clamps with a superglue. The resulting specimens have a size of 10 mm × 10 mm × 1 mm (length × width × thickness). Uniaxial tensile tests were performed using an Instron 5543 universal testing machine with a 1000 N load cell at 25 °C in air. The specimens were stretched at a rate of 5 mm/min until the samples were broken. The elastic modulus and toughness were calculated from the initial slope (strain range of 10−30%) and the area under the stress−strain curve, respectively. Each film type was tested in quintuplicate; the average and standard deviations from this set were plotted. Micromorphology of the dried hydrogel film was observed using a Carl Zeiss SUPRA 55VP scanning electron microscope at an accelerating voltage of 2 kV. Before the measurement, the sample was dried using a lyophilizer for 3 d and coated with a thin platinum layer. Attenuated total reflection Fourier transform infrared spectroscopy measurements were performed using a Nicolet-6700 instrument (Thermo Scientific) at room temperature. The spectrum was obtained by averaging 32 scans over the range of 4000 to 400 cm^{-1}.

Synthesis of a Poly(acrylic acid)-Based Hydrogel. Hydrogel films were prepared via typical free-radical polymerization. A representative example of hydrogel **2** was prepared as follows: To a solution of acrylic acid (14.7 g, 0.204 mol, 1490 equiv) in water (8 mL), sodium hydroxide (6.6 g, 0.165 mol, 1190 equiv) was added dropwise in water (16 mL), resulting in 80% neutralization of acrylic acid. The monomer solution was degassed by vigorous N_2 bubbling for 1 h. After adding KPS (37 mg, 0.14 mmol, 1.0 equiv, 0.25 wt %) and di(ethylene glycol) diacrylate (50 mg, 0.23 mmol, 1.7 equiv, 0.34 wt %), the reaction mixture was transferred to a glass template having a size of 11.5 cm × 15 cm × 0.1 cm (width × length × thickness) and placed on a heating plate having a set temperature of 55 °C for 2 h. A freestanding hydrogel film was obtained after unloading from the mold in a quantitative yield. IR (cm^{-1}): 3361, 2932, 2852, 1685.8, 1552, 1405, 1294; ^{1}H NMR (300 MHz, D_2O): δ 1.82 (br s, methine protons), 1.23 (br s, methylene protons); ^{13}C NMR (125 MHz, D_2O): δ 183.6, 44.8, 37.3, 36.1. The obtained NMR spectra are shown in Figures S9 and S10. The amounts of initiator and cross-linker were varied from 0.05 to 0.75 and from 0.20 to 0.80 wt %, respectively, with reference to the amount of acrylic acid monomer. For investigating the cross-linker effect (Figure 4), the amount of initiator was set at 0.25 wt %; for the initiator effect (Figure S1), 0.34 wt % cross-linker was used, as shown in Table 2.

Preparation of Bilayered Hydrogels. Bilayered hydrogels were prepared by sequential radical polymerization. Di(ethylene glycol)diacrylate (50 mg, 0.233 mmol, 1.7 equiv, 0.34 wt %), KPS (37 mg, 0.14 mmol, 1.0 equiv, 0.25 wt %), and a navy blue dye (10 mg) were added to 80%-neutralized acrylic acid (14.7 g, 0.204 mol, 1490 equiv) solution. The first polymerizing solution was poured into a glass template (11.5 cm × 15 cm × 0.1 cm), which was covered with a glass lid, and

DOI: 10.1021/acsomega.8b00079
ACS Omega 2018, 3, 3096−3103

Table 2. Compositions of Cross-Linker and Initiator Incorporated in Hydrogel Films for Tensile Testing

for cross-linker effect		for initiator effect		
cross-linker (wt %)	initiator (wt %)	cross-linker (wt %)	initiator (wt %)	control variables
0.20	0.25	0.34	0.05	acrylic acid NaOH water
0.34			0.17	
0.42			0.25	
0.50			0.43	
0.63			0.56	
0.80			0.75	

heated at 55 °C for 2 h to afford the first layer. The second layer was synthesized onto the first layer in a similar manner. After the fabrication of the first layer inside the glass template, additional glass slides (thickness, 0.1 cm) were placed as a spacer. In this step, the first layer was masked with glass pieces when preparing the patterned bilayer. The second polymerizing solution was prepared by adding di(ethylene glycol)diacrylate (119 mg, 0.556 mmol, 4.1 equiv, 0.80 wt %), KPS (37 mg, 0.14 mmol, 1.0 equiv, 0.25 wt %), and a red dye (10 mg) to the 80%-neutralized acrylic acid solution. The second solution was carefully injected into the gap between the first layer and glass lid and then heated at 55 °C for 2 h. The freestanding bilayer hydrogel was obtained in a quantitative yield after unloading from the mold and cut into pieces of desired sizes by using a laser cutter or razor.

■ ASSOCIATED CONTENT

Supporting Information

The Supporting Information is available free of charge on the ACS Publications website at DOI: 10.1021/acsomega.8b00079.

Materials, instrumentation, experimental details, characterization data, and ^{1}H and ^{13}C NMR spectra (PDF)

■ AUTHOR INFORMATION

Corresponding Authors

*E-mail: jichang@snu.ac.kr (J.Y.C).
*E-mail: kimhw@jnu.ac.kr (H.K.).

ORCID

Hyungwoo Kim: 0000-0003-1958-3587

Notes

The authors declare no competing financial interest.

■ ACKNOWLEDGMENTS

This work was supported by the National Research Foundation of Korea (NRF) grant funded by the Korean government (MSIP) (nos. 2017R1C1B5017785 and 2015R1A2A2A01006585) and by Research and Business Development Program through the Ministry of Trade, Industry and Energy (MOTIE) and the Korea Institute for Advancement of Technology (KIAT) (no. N0002439). Financial support from LG Chem. Ltd. is also acknowledged.

■ REFERENCES

(1) Wichterle, O.; Lím, D. Hydrophilic gels for biological use. *Nature* **1960**, *185*, 117−118.

(2) Rodrigues, F. H. A.; Spagnol, C.; Pereira, A. G. B.; Martins, A. F.; Fajardo, A. R.; Rubira, A. F.; Muniz, E. C. Superabsorbent hydrogel composites with a focus on hydrogels containing nanofibers or nanowhiskers of cellulose and chitin. *J. Appl. Polym. Sci.* **2014**, *131*, 39725.

(3) Guilherme, M. R.; Aouada, F. A.; Fajardo, A. R.; Martins, A. F.; Paulino, A. T.; Davi, M. F. T.; Rubira, A. F.; Muniz, E. C. Superabsorbent hydrogels based on polysaccharides for application in agriculture as soil conditioner and nutrient carrier: A review. *Eur. Polym. J.* **2015**, *72*, 365−385.

(4) Ullah, F.; Othman, M. B. H.; Javed, F.; Ahmad, Z.; Akil, H. M. Classification, processing and application of hydrogels: A review. *Mater. Sci. Eng., C* **2015**, *57*, 414−433.

(5) Kollár, J.; Mrlík, M.; Moravčíková, D.; Kroneková, Z.; Liptaj, T.; Lacík, I.; Mosnáček, J. Tulips: A Renewable Source of Monomer for Superabsorbent Hydrogels. *Macromolecules* **2016**, *49*, 4047−4056.

(6) Kabiri, K.; Omidian, H.; Zohuriaan-Mehr, M. J.; Doroudiani, S. Superabsorbent hydrogel composites and nanocomposites: A review. *Polym. Compos.* **2011**, *32*, 277−289.

(7) Kelly, J. A.; Shukaliak, A. M.; Cheung, C. C. Y.; Shopsowitz, K. E.; Hamad, W. Y.; MacLachlan, M. J. Responsive Photonic Hydrogels Based on Nanocrystalline Cellulose. *Angew. Chem., Int. Ed.* **2013**, *52*, 8912−8916.

(8) Kettunen, M.; Silvennoinen, R. J.; Houbenov, N.; Nykänen, A.; Ruokolainen, J.; Sainio, J.; Pore, V.; Kemell, M.; Ankerfors, M.; Lindström, T.; Ritala, M.; Ras, R. H. A.; Ikkala, O. Photoswitchable Superabsorbency Based on Nanocellulose Aerogels. *Adv. Funct. Mater.* **2011**, *21*, 510−517.

(9) Lu, T.; Xiang, T.; Huang, X.-L.; Li, C.; Zhao, W.-F.; Zhang, Q.; Zhao, C.-S. Post-crosslinking towards stimuli-responsive sodium alginate beads for the removal of dye and heavy metals. *Carbohydr. Polym.* **2015**, *133*, 587−595.

(10) Haseeb, M. T.; Hussain, M. A.; Yuk, S. H.; Bashir, S.; Nauman, M. Polysaccharides based superabsorbent hydrogel from Linseed: Dynamic swelling, stimuli responsive on−off switching and drug release. *Carbohydr. Polym.* **2016**, *136*, 750−756.

(11) Deligkaris, K.; Tadele, T. S.; Olthuis, W.; van den Berg, A. Hydrogel-based devices for biomedical applications. *Sens. Actuators, B* **2010**, *147*, 765−774.

(12) Chan, A. W.; Whitney, R. A.; Neufeld, R. J. Semisynthesis of a Controlled Stimuli-Responsive Alginate Hydrogel. *Biomacromolecules* **2009**, *10*, 609−616.

(13) Shi, X.; Wang, W.; Zheng, Y.; Wang, A. Utilization of hollow kapok fiber for the fabrication of a pH-sensitive superabsorbent composite with improved gel strength and swelling properties. *RSC Adv.* **2014**, *4*, 50478−50485.

(14) Gao, Y.; Li, X.; Serpe, M. J. Stimuli-responsive microgel-based etalons for optical sensing. *RSC Adv.* **2015**, *5*, 44074−44087.

(15) Chen, F.; Greiner, A.; Agarwal, S. Stimuli-Responsive Elastic Polyurethane-Based Superabsorber Nanomat Composites. *Macromol. Mater. Eng.* **2011**, *296*, 517−523.

(16) Wang, W.; Wang, A. Preparation, swelling, and stimuli-responsive characteristics of superabsorbent nanocomposites based on carboxymethyl cellulose and rectorite. *Polym. Adv. Technol.* **2011**, *22*, 1602−1611.

(17) Chang, C.; Zhang, L. Cellulose-based hydrogels: Present status and application prospects. *Carbohydr. Polym.* **2011**, *84*, 40−53.

(18) Tang, S.; Floy, M.; Bhandari, R.; Sunkara, M.; Morris, A. J.; Dziubla, T. D.; Hilt, J. Z. Synthesis and Characterization of Thermoresponsive Hydrogels Based on *N*-Isopropylacrylamide Cross-linked with 4,4′-Dihydroxybiphenyl Diacrylate. *ACS Omega* **2017**, *2*, 8723−8729.

(19) Matsumoto, H.; Seto, H.; Akiyoshi, T.; Shibuya, M.; Hoshino, Y.; Miura, Y. Macroporous Gel with a Permeable Reaction Platform for Catalytic Flow Synthesis. *ACS Omega* **2017**, *2*, 8796−8802.

(20) Ahiabu, A.; Serpe, M. J. Rapidly Responding pH- and Temperature-Responsive Poly (N-Isopropylacrylamide)-Based Microgels and Assemblies. *ACS Omega* **2017**, *2*, 1769−1777.

(21) Jiao, T.; Zhao, H.; Zhou, J.; Zhang, Q.; Luo, X.; Hu, J.; Peng, Q.; Yan, X. Self-Assembly Reduced Graphene Oxide Nanosheet Hydrogel Fabrication by Anchorage of Chitosan/Silver and Its Potential Efficient

DOI: 10.1021/acsomega.8b00079
ACS Omega 2018, 3, 3096−3103

Application toward Dye Degradation for Wastewater Treatments. *ACS Sustainable Chem. Eng.* **2015**, *3*, 3130−3139.
(22) Chen, F.; Guo, J.; Xu, D.; Yan, F. Thermo- and pH-responsive poly(ionic liquid) membranes. *Polym. Chem.* **2016**, *7*, 1330−1336.
(23) Gao, L.; Guo, G.; Liu, M.; Tang, Z.; Xie, L.; Huo, Y. Multi-responsive, bidirectional, and large deformation bending actuators based on borax cross-linked polyvinyl alcohol derivative hydrogel. *RSC Adv.* **2017**, *7*, 40005−40014.
(24) Jia, H.; Huang, Z.; Fei, Z.; Dyson, P. J.; Zheng, Z.; Wang, X. Bilayered polyurethane/dipole−dipole and H-bonding interaction reinforced hydrogels as thermo-responsive soft manipulators. *J. Mater. Chem. B* **2017**, *5*, 8193−8199.
(25) Chen, Y.-N.; Peng, L.; Liu, T.; Wang, Y.; Shi, S.; Wang, H. Poly(vinyl alcohol)−Tannic Acid Hydrogels with Excellent Mechanical Properties and Shape Memory Behaviors. *ACS Appl. Mater. Interfaces* **2016**, *8*, 27199−27206.
(26) Yang, F.; Sukhishvili, S.; Du, H.; Tian, F. Marine salinity sensing using long-period fiber gratings enabled by stimuli-responsive polyelectrolyte multilayers. *Sens. Actuators, B* **2017**, *253*, 745−751.
(27) Lee, B. P.; Narkar, A.; Wilharm, R. Effect of metal ion type on the movement of hydrogel actuator based on catechol-metal ion coordination chemistry. *Sens. Actuators, B* **2016**, *227*, 248−254.
(28) Wu, S.; Yu, F.; Dong, H.; Cao, X. A hydrogel actuator with flexible folding deformation and shape programming via using sodium carboxymethyl cellulose and acrylic acid. *Carbohydr. Polym.* **2017**, *173*, 526−534.
(29) Peng, K.; Yang, K.; Fan, Y.; Yasin, A.; Hao, X.; Yang, H. Thermal/Light Dual-Activated Shape Memory Hydrogels Composed of an Agarose/Poly(acrylamide-co-acrylic acid) Interpenetrating Network. *Macromol. Chem. Phys.* **2017**, *218*, 1700170.
(30) Yang, C.; Liu, Z.; Chen, C.; Shi, K.; Zhang, L.; Ju, X.-J.; Wang, W.; Xie, R.; Chu, L.-Y. Reduced Graphene Oxide-Containing Smart Hydrogels with Excellent Electro-Response and Mechanical Properties for Soft Actuators. *ACS Appl. Mater. Interfaces* **2017**, *9*, 15758−15767.
(31) Takada, K.; Iida, T.; Kawanishi, Y.; Yasui, T.; Yuchi, A. An electrochemical actuator based on reversible changes in volume of poly(acrylic acid) gel induced by quinone redox. *Sens. Actuators, B* **2011**, *160*, 1586−1592.
(32) Browe, D. P.; Wood, C.; Sze, M. T.; White, K. A.; Scott, T.; Olabisi, R. M.; Freeman, J. W. Characterization and optimization of actuating poly(ethylene glycol) diacrylate/acrylic acid hydrogels as artificial muscles. *Polymer* **2017**, *117*, 331−341.
(33) Bryant, S. J.; Chowdhury, T. T.; Lee, D. A.; Bader, D. L.; Anseth, K. S. Crosslinking density influences chondrocyte metabolism in dynamically loaded photocrosslinked poly(ethylene glycol) hydrogels. *Ann. Biomed. Eng.* **2004**, *32*, 407−417.
(34) Mudiyanselage, T. K.; Neckers, D. C. Highly Absorbing Superabsorbent Polymer. *J. Polym. Sci., Part A: Polym. Chem.* **2008**, *46*, 1357−1364.
(35) O'Neil, G. A.; Wisnudel, M. B.; Torkelson, J. M. A Critical Experimental Examination of the Gel Effect in Free Radical Polymerization: Do Entanglements Cause Autoacceleration? *Macromolecules* **1996**, *29*, 7477−7490.
(36) Chen, J.; Zhao, Y. Relationship Between Water Absorbency and Reaction Conditions in Aqueous Solution Polymerization of Polyacrylate Superabsorbents. *J. Appl. Polym. Sci.* **2000**, *75*, 808−814.
(37) Singhal, R.; Tomar, R. S.; Nagpal, A. K. Effect of cross-linker and initiator concentration on the swelling behaviour and network parameters of superabsorbent hydrogels based on acrylamide and acrylic acid. *Int. J. Plast. Technol.* **2009**, *13*, 22−37.
(38) Odian, G. *Principles of Polymerization*, 4th ed.; John Wiley & Sons, Inc.: New York, 2004.
(39) Wong, K. K. H.; Zinke-Allmang, M.; Wan, W. Effect of annealing on aqueous stability and elastic modulus of electrospun poly(vinyl alcohol) fibers. *J. Mater. Sci.* **2010**, *45*, 2456−2465.
(40) Xing, B.; Yu, C.-W.; Chow, K.-H.; Ho, P.-L.; Fu, D.; Xu, B. Hydrophobic Interaction and Hydrogen Bonding Cooperatively Confer a Vancomycin Hydrogel: A Potential Candidate for Biomaterials. *J. Am. Chem. Soc.* **2002**, *124*, 14846−14847.

DOI: 10.1021/acsomega.8b00079
ACS Omega 2018, 3, 3096−3103